Table 3 Adverse events (AEs) observed during the study

	12.5 mg ($N = 12$)	25 mg ($N = 14$)	37.5 mg ($N = 12$)
Adverse events with ≥2 patients in any group, *n* (%)	6 (50 %)	7 (50 %)	9 (75 %)
Back pain	1 (8 %)	0	4 (33 %)
Pyrexia	0	3 (21 %)	2 (17 %)
Postoperative fever	3 (25 %)	0	2 (17 %)
Pleural effusion	2 (17 %)	0	2 (17 %)
Abdominal distension	1 (8 %)	0	2 (17 %)
Ascites	1 (8 %)	0	2 (17 %)
Procedural pain	2 (17 %)	0	1 (8 %)
ALT increased	2 (17 %)	1 (7 %)	0
AST increased	2 (17 %)	1 (7 %)	0
All grade 3 or 4 adverse events, *n* (%)	0	0	1 (8 %)
All drug-related adverse events, *n* (%)	1 (8 %)	4 (29 %)	4 (33 %)
Diarrhea	0	1 (7 %)	1 (8 %)
Renal impairment	0	1 (7 %)	1 (8 %)
Abdominal distension	0	0	1 (8 %)
Abdominal pain	0	0	1 (8 %)
Back pain	0	0	1 (8 %)
Eosinophilia	0	0	1 (8 %)
Eosinophil count increased	0	0	1 (8 %)
Anorexia	0	0	1 (8 %)
Pleural effusion	0	0	1 (8 %)
Pain in extremity	0	1 (7 %)	0
Vomiting	0	1 (7 %)	0
Urinary tract infection	0	1 (7 %)	0
Supraventricular extrasystoles	1 (8 %)	0	0
Serious adverse events, *n* (%)	0	0	2 (17 %)
Ascites	0	0	1 (8 %)
Pleural effusion	0	0	1[a] (8 %)
Portal vein thrombosis	0	0	1[a] (8 %)
Death, *n* (%)	0	0	1[b] (8 %)

The severity of adverse events was graded using the Division of AIDS Table for Grading the Severity of Adult and Pediatric Adverse Events (version 1.9, dated December 2004). The data include AEs seen on study plus all drug-related AEs

ALT alanine aminotransferase, *AST* aspartate aminotransferase

[a] One patient experienced pleural effusion and portal vein thrombosis 22 days post-treatment

[b] The death occurred 149 days after the end of treatment with eltrombopag

possibilities may account for this difference. First, plasma eltrombopag concentrations in patients with CLD are higher than those in patients with ITP [21, 26], and therefore the differences in exposure between these 2 diseases may be responsible for changes in platelet counts after treatment with eltrombopag. Second, the difference may be based on the pathogenesis of thrombocytopenia. The main cause of thrombocytopenia in patients with ITP is an autoimmune-mediated active platelet destruction. In patients with CLD, increased blood flow into the spleen secondary to portal hypertension and subsequent passive trapping of platelets in the spleen contribute to thrombocytopenia in this patient population [31, 32].

Most AEs reported in the present study were grade 1 or 2 in severity, and no significant aminotransferase abnormalities were observed. The incidence of drug-related AEs in the 37.5 mg group was somewhat higher compared with the other groups, and drug-related serious events (ascites, increase of pleural effusion, and development of portal vein thrombosis) were seen in 2 patients receiving 37.5 mg of eltrombopag. There was 1 portal vein thrombosis event seen after eltrombopag treatment. Post-hoc analyses of a study of non-Japanese patients with CLD and thrombocytopenia receiving 75 mg of eltrombopag showed that maximum post-baseline platelet counts were associated with the thromboses observed in that study [33]. Thus, thrombogenesis seems to be a factor for the development of the thrombotic events. In addition, it has recently been reported that platelets can amplify inflammation [34], suggesting that platelet-amplified inflammation could be a possible factor for the development of thrombosis. The minimum effective dose of eltrombopag should therefore be used in order to minimize the risk of thromboembolic events, and platelet counts should be closely monitored.

It may be unusual to recommend an optimal dose of eltrombopag in Japanese patients with CLD based only on this study. Nevertheless, we propose that 12.5 or 25 mg can be recommended for Japanese patients with CLD and thrombocytopenia undergoing invasive procedures, based on the following 3 findings: (1) a higher mean concentration of eltrombopag was observed in patients with Child–Pugh class B compared with Child–Pugh class A in the 37.5 mg group (Fig. 2); (2) although the mean $AUC_{0-\tau}$ increased with an increase in the eltrombopag dose, the increase in platelet counts seemed to be saturated at 25 mg of eltrombopag (Figs. 3, 4); (3) SAEs were seen in the 37.5 mg group. Although the SAEs may have been due in part to invasive procedures or the natural course of the disease, we could not rule out the possibility of these being drug-related.

In our study, except for 1 patient treated with partial hepatectomy, splenectomy, and cholecystectomy, perioperative bleeding was not seen and platelet transfusions were not required before invasive procedures. These findings suggested that eltrombopag may reduce the necessity for platelet transfusions in patients with CLD undergoing invasive procedures.

These findings demonstrated that a maximum daily dose of 25 mg of eltrombopag administered for 2 weeks was

Table 4 Effects of pretreatment with eltrombopag on the prevalence of perioperative bleeding and platelet transfusions

Groups	Case number	Procedure	Bleeding	Platelet transfusion	Days after end of treatment	Platelet count (/μL)		
						Baseline	Pre-procedure	Post-procedure
12.5 mg	11	Partial hepatectomy, splenectomy, cholecystectomy	Yes	Yes[a]	8	42,000	46,000	194,000
	31	Radiofrequency ablation	No	No	3	43,000	173,000	178,000
25 mg	5	Radiofrequency ablation	No	No	13	48,000	217,000	152,000
	6	Tooth extraction	No	No	9	45,000	387,000	382,000
		Tooth extraction	No	No	13	45,000	387,000	382,000
	32	Liver biopsy	No	No	1	46,000	146,000	142,000
37.5 mg	51	Radiofrequency ablation	No	No	6	37,000	126,000	183,000

[a] Platelet transfusion was performed prior to invasive procedures

effective and well-tolerated for Japanese patients with CLD. Eltrombopag seems to be an efficacious alternative to platelet transfusions for supporting invasive procedures in patients with CLD and thrombocytopenia, although there might be a risk of treatment-related thrombosis. Further studies will help to establish the appropriate use of eltrombopag for supporting invasive procedures in patients with CLD and thrombocytopenia while investigating the effective prevention of thrombosis.

In conclusion, eltrombopag ameliorated thrombocytopenia in Japanese patients with CLD. A daily dose of 25 mg and 2-week administration is recommended for these patients. Recently, Afdhal et al. [35] reported that patients with HCV who were treated with eltrombopag showed significantly higher sustained virologic response rates following interferon-based therapy compared with patients treated with placebo. Therefore, in addition to its role as a supporting agent for invasive procedures, further studies will be focused on the ability of eltrombopag to initiate and maintain the interferon therapy, and subsequently facilitate an increase in the sustained virologic response rate in patients with thrombocytopenia with chronic HCV infection.

Acknowledgments This study was supported by GlaxoSmithKline, Tokyo, Japan. The authors thank the patients, physicians, nurses, and study coordinators who participated in the study. We also thank the following GlaxoSmithKline employees for their assistance in statistical analysis, interpretation of data, and preparation of this manuscript: Takumi Terao, Naoki Takahashi, and Yuki Matsuzawa.

Conflict of interest Toshihiro Hattori and Koichi Katsura are employees of GlaxoSmithKline, Tokyo, Japan. All other authors declare no conflict of interest.

References

1. Lu SN, Wang JH, Liu SL, Hung CH, Chen CH, Tung HD, et al. Thrombocytopenia as a surrogate for cirrhosis and a marker for the identification of patients at high-risk for hepatocellular carcinoma. Cancer. 2006;107:2212–22.
2. Afdhal N, McHutchison J, Brown R, Jacobson I, Manns M, Poordad F, et al. Thrombocytopenia associated with chronic liver disease. J Hepatol. 2008;48:1000–7.
3. Rios R, Sangro B, Herrero I, Quiroga J, Prieto J. The role of thrombopoietin in the thrombocytopenia of patients with liver cirrhosis. Am J Gastroenterol. 2005;100:1311–6.
4. British Committee for Standards in Haematology, Blood Transfusion Task Force. Guidelines for the use of platelet transfusions. Br J Haematol. 2003;122:10–23.
5. Samama CM, Djoudi R, Lecompte T, Nathan-Denizot N, Jean-François F, Agence Française de Sécurité Sanitaire des Produits de Santé expert group, et al. Perioperative platelet transfusion: recommendations of the Agence française de Sécurité Sanitaire des Produits De Santé (AFSSaPS) 2003. Can J Anesth. 2006;72:447–52.
6. Norfolk DR, Ancliffe PJ, Contreras M, Hunt BJ, Machin SJ, Murphy WG, et al. Consensus conference on platelet transfusion, Royal College of Physicians of Edinburgh 27–28 November 1997. Br J Haematol. 1998;101:609–17.
7. Rebulla P. Revisitation of the clinical indications for the transfusion of platelet concentrates. Rev Clin Exp Hematol. 2001;5:288–310.
8. Rebulla P. Platelet transfusion trigger in difficult patients. Transfus Clin Biol. 2001;8:249–54.
9. Eisen GM, Baron TH, Dominitz JA, Faigel DO, Goldstein JL, Johanson JF, et al. Complications of upper GI endoscopy. Gastrointest Endosc. 2002;55:784–93.
10. Kawaguchi T, Kuromatsu R, Ide T, Taniguchi E, Itou M, Sakata M, et al. Thrombocytopenia, an important interfering factor of antiviral therapy and hepatocellular carcinoma treatment for chronic liver diseases. Kurume Med J. 2009;56:9–15.
11. Eder AF, Chambers LA. Noninfectious complications of blood transfusions. Arch Pathol Lab Med. 2007;131:708–18.
12. Wilhelm D, Klouche M, Fiebelkorn A, Görg S, Klüter H, Kirchner H. Non-haemolytic transfusion reactions after platelet substitution. Lancet. 1993;342:364.
13. Vamvakas EC. Platelet transfusion and adverse outcomes. Lancet. 2004;364:1736–8.

14. Okabayashi T, Hanazaki K. Overwhelming postsplenectomy infection syndrome in adults—a clinically preventable disease. World J Gastroenterol. 2008;14:176–9.
15. Stasi R, Evangelista ML, Amadori S. Novel thrombopoietic agents a review of their use in idiopathic thrombocytopenic purpura. Drugs. 2008;68:901–12.
16. Matthys G, Park JW, McGuire S, Wire MB, Bowen C, Williams D, et al. Clinical pharmacokinetics, platelet response, and safety of eltrombopag at supratherapeutic doses of up to 200 mg once daily in healthy volunteers. J Clin Pharmacol. 2011;51(3):301–8 (Epub 2010 Apr 23).
17. Bussel JB, Cheng G, Saleh MN, Psaila B, Kovaleva L, Meddeb B, et al. Eltrombopag for the treatment of chronic idiopathic thrombocytopenic purpura. N Engl J Med. 2007;357:2237–47.
18. McHutchison JG, Dusheiko G, Shiffman ML, Rodriguez-Torres M, Sigal S, Bourliere M, et al. Eltrombopag for thrombocytopenia in patients with cirrhosis associated with hepatitis C. N Engl J Med. 2007;357:2227–36.
19. Cheng G, Saleh MN, Marcher C, Vasey S, Mayer B, Aivado M, et al. Eltrombopag for management of chronic immune thrombocytopenia (RAISE): a 6-month, randomized, phase 3 study. Lancet. 2011;377:393–402.
20. Bauman JW, Vincent CT, Peng B, Wire MB, Williams DD, Park JW. Effect of hepatic or renal impairment on eltrombopag pharmacokinetics. J Clin Pharmacol. 2011;51:739–50.
21. Gibiansky E, Zhang J, Williams D, Wang Z, Ouellet D. Population pharmacokinetics of eltrombopag in healthy subjects and patients with chronic idiopathic thrombocytopenic purpura. J Clin Pharmacol. 2011;51:842–56.
22. Heddle NM, Cook RJ, Tinmouth A, Kouroukis CT, Hervig T, Klapper E, et al. A randomized controlled trial comparing standard- and low-dose strategies for transfusion of platelets (SToP) to patients with thrombocytopenia. Blood. 2009;113:1564–73.
23. Wai CT, Greenson JK, Fontana RJ, Kalbfleisch JD, Marrero JA, Conjeevaram HS, et al. A simple noninvasive index can predict both significant fibrosis and cirrhosis in patients with chronic hepatitis C. Hepatology. 2003;38(2):518–26.
24. The Japanese Society of Gastroenterology, editor. Liver cirrhosis practical guideline. Tokyo: Nankodo Co. Ltd.; 2009.
25. Drinka PJ, Langer E. The Cockroft–Gault formula. J Am Geriatr Soc. 1989;37(8):820.
26. Farrell C, Hayes S, Giannini EG, Afdhal NH, Tayyab GN, Mohsin A, et al. Gender, race, and severity of liver disease influence eltrombopag exposure in thrombocytopenic patients with chronic liver disease. Hepatology. 2010;52:920A.
27. Shida Y, Takahashi N, Nohda S, Hirama T. Pharmacokinetics and pharmacodynamics of eltrombopag in healthy Japanese males. Jpn J Clin Pharmacol Ther. 2011;42:11–20.
28. Zhang A, Xing Q, Qin S, Du J, Wang L, Yu L, et al. Intra-ethnic differences in genetic variants of the UGT-glucuronosyltransferase 1A1 gene in Chinese populations. Pharmacogenomics J. 2007;7:333–8.
29. Mizutani T. PM frequencies of major CYPs in Asians and Caucasians. Drug Metab Rev. 2003;35:99–106.
30. Afdhal N, Giannini E, Tayyab GN, Mohsin A, Lee JW, Andriulli A, et al. Eltrombopag in chronic liver disease patients with thrombocytopenia undergoing an elective procedure: results from ELEVATE, a randomized clinical trial. J Hepatol. 2010;52:S460 (Abstr 1185).
31. Cines DB, Blanchette V. Immune thromocytopenic purpura. N Engl J Med. 2002;346:995–1008.
32. Giannini EG, Savarino V. Thrombocytopenia in liver disease. Curr Opin Hematol. 2008;15:473–80.
33. Giannini EG, Afdal NH, Campbell FM, Blackman NJ, Shi W, Hyde DK, et al. Exploratory analyses of predictors of thrombotic events in the ELEVATE study. Hepatology. 2010;52:1071A (Abstr 1569).
34. Boilard E, Nigrovic PA, Larabee K, Watts GFM, Ciblyn JS, Weinblatte ME, et al. Platelets amplify inflammation in arthritis via collagen-dependent microparticle production. Science. 2010;327:580–3.
35. Afdhal N, Dusheiko G, Giannini EG, Chen P, Han K, Moshin A, et al. Final results of ENABLE 1, a phase 3, multicenter study of eltrombopag as an adjunct for antiviral treatment of hepatitis C virus-related chronic liver disease associated with thrombocytopenia. Hepatology. 2011;54:1427A–28A (LB-3 Abstract form).

Aging Cell (2012) **11**, pp553–556 Doi: 10.1111/j.1474-9726.2012.00809.x

SHORT TAKE

Quantitative assessment of higher-order chromatin structure of the *INK4/ARF* locus in human senescent cells

Akiyuki Hirosue,[1,2] Ko Ishihara,[3] Kazuaki Tokunaga,[1] Takehisa Watanabe,[1] Noriko Saitoh,[1] Masafumi Nakamoto,[1] Tamir Chandra,[4,5] Masashi Narita,[4,5] Masanori Shinohara[2] and Mitsuyoshi Nakao[1]

[1]Department of Medical Cell Biology, Institute of Molecular Embryology and Genetics, Global Center of Excellence 'Cell Fate Regulation Research and Education Unit', Kumamoto University, Kumamoto 860-0811, Japan
[2]Department of Oral and Maxillofacial Surgery, Faculty of Life Sciences, Kumamoto University, Kumamoto 860-8556, Japan
[3]Priority Organization for Innovation and Excellence, Kumamoto University, Kumamoto 860-0811, Japan
[4]Cancer Research UK, Cambridge Research Institute, Li Ka Shing Centre, Cambridge CB2 0RE, UK
[5]Department of Oncology, University of Cambridge, Cambridge CB2 0RE, UK

Summary

Somatic cells can be reset to oncogene-induced senescent (OIS) cells or induced pluripotent stem (iPS) cells by expressing specified factors. The *INK4/ARF* locus encodes $p15^{INK4b}$, *ARF*, and $p16^{INK4a}$ genes in human chromosome 9p21, the products of which are known as common key reprogramming regulators. Compared with growing fibroblasts, the CCCTC-binding factor CTCF is remarkably up-regulated in iPS cells with silencing of the three genes in the locus and is reversely down-regulated in OIS cells with high expression of $p15^{INK4b}$ and $p16^{INK4a}$ genes. There are at least three CTCF-enriched sites in the *INK4/ARF* locus, which possess chromatin loop-forming activities. These CTCF-enriched sites and the $p16^{INK4a}$ promoter associate to form compact chromatin loops in growing fibroblasts, while CTCF depletion disrupts the loop structure. Interestingly, the loose chromatin structure is found in OIS cells. In addition, the *INK4/ARF* locus has an intermediate type of chromatin compaction in iPS cells. These results suggest that senescent cells have distinct higher-order chromatin signature in the *INK4/ARF* locus.

Key words: chromatin organization; CTCF; *INK4/ARF*; senescent cells; stem cells.

Somatic fibroblasts can be reprogrammed to senescent cells by oncogenic activation (Serrano *et al.*, 1997) or to induced pluripotent stem (iPS) cells by the expression of transcription factors associated with pluripotency (Takahashi *et al.*, 2007). The *INK4/ARF* locus, which encodes $p15^{INK4b}$, $p16^{INK4a}$, and *ARF* genes (Gil & Peters, 2006; Kim & Sharpless, 2006), is an inducer of senescence (Collado *et al.*, 2007) and a barrier for reprogramming into iPS cells (Banito *et al.*, 2009; Li *et al.*, 2009). In fact, the conversion to iPS cells is strongly impaired by senescent program. The CCCTC-binding factor CTCF is known to possess essential functions including transcriptional control, chromatin insulation, and chromosomal interactions within the three-dimensional context of the nucleus (Phillips & Corces, 2009; Ohlsson *et al.*, 2010).

Here, we analyzed the role of CTCF in well-established human cell lines: 201B7 cells, induced from fibroblasts and recognized as the iPS cell standard, human diploid fibroblasts (IMR90), and the same cells undergoing oncogene-induced senescence after Ras activation (oncogene-induced senescent, OIS) (Fig. S1, Supporting information). To avoid the variability between the cells, we used early passage IMR90 cells (Narita *et al.*, 2003) and repeated experiments in other cell lines such as 253G1 cells for iPS cells. Interestingly, *CTCF* mRNA was remarkably up-regulated in iPS cells and reversely down-regulated in OIS cells, compared with that of IMR90 cells (Fig. 1A). We also found increased CTCF protein in iPS cells, but decreased levels of expression in senescent cells (Fig. S2, Supporting information). Using the same samples, $p15^{INK4b}$, *ARF*, and $p16^{INK4a}$ were significantly silenced in iPS cells and IMR90 cells (Fig. 1A and Fig. S2, Supporting information). In contrast, as previously shown, $p15^{INK4b}$ and $p16^{INK4a}$ were up-regulated in OIS cells (day 6), with no change in the expression of *ARF*.

Using genome-wide CTCF-binding profiles available at the websites and our published data (Wendt *et al.*, 2008; Mishiro *et al.*, 2009), there were at least three CTCF-enriched sites in this locus, named IC1, IC2, and IC3 (Fig. S3, Supporting information). IC1 and IC2 were downstream of the $p15^{INK4b}$ and *ARF* transcription start sites, respectively, while IC3 was downstream of $p16^{INK4a}$ exon 3. Chromatin immunoprecipitation showed that CTCF bound to IC1, IC2, and IC3 sites in all three cell lines (Fig. 1B), but did not bind to $p16^{INK4a}$ exon 1 as a negative control (data not shown). Compared with IMR90 cells, the amount of CTCF decreased at IC1 and IC3 sites in OIS cells. In contrast, CTCF binding was significantly high in iPS cells.

Using a chromosome conformation capture (3C) assay, we measured the interaction frequencies of the reference IC1/$p15^{INK4b}$ with nine distinct *Eco*RI fragments in the locus in IMR90 cells (Fig. 1C). The IC1 site was colocalized with IC2/*ARF*, the $p16^{INK4a}$ promoter, and IC3 (red line). The IC2/*ARF* reference strongly interacted with IC1/$p15^{INK4b}$ (Fig. 1D). Further, interaction frequencies of the IC3 reference increased at IC1/$p15^{INK4b}$ (Fig. 1E). These data indicate that IC1/$p15^{INK4b}$, IC2/*ARF*, the $p16^{INK4}$ promoter, and IC3 are closely localized in nuclei, leading to possible formation of chromatin loops in the *INK4/ARF* locus (as modeled in Fig. 2D). Importantly, CTCF knockdown decreased their colocalization (purple line), resulting in increased expression of $p15^{INK4b}$ and $p16^{INK4a}$ (Fig. S4A–D, Supporting information). The depletion of the cofactor cohesin RAD21 (Wendt *et al.*, 2008), which coexisted with CTCF at the IC sites, also induced the *INK4/ARF* genes (Fig. S4E–G, Supporting information). These data suggest that CTCF complex is involved in the compact chromatin formation at the *INK4/ARF* locus.

We then performed a 3C assay in IMR90, OIS, and iPS cells (Fig. 2). Using three reference sites (yellow bars), the IC sites and the $p16^{INK4a}$ pro-

Correspondence
Mitsuyoshi Nakao, Department of Medical Cell Biology, Institute of Molecular Embryology and Genetics, Kumamoto University, 2-2-1 Honjo, Kumamoto 860-0811, Japan. Tel: +81 96 373 6800; fax: +81 96 373 6804; e-mail: mnakao@gpo.kumamoto-u.ac.jp

Accepted for publication *7 February 2012*

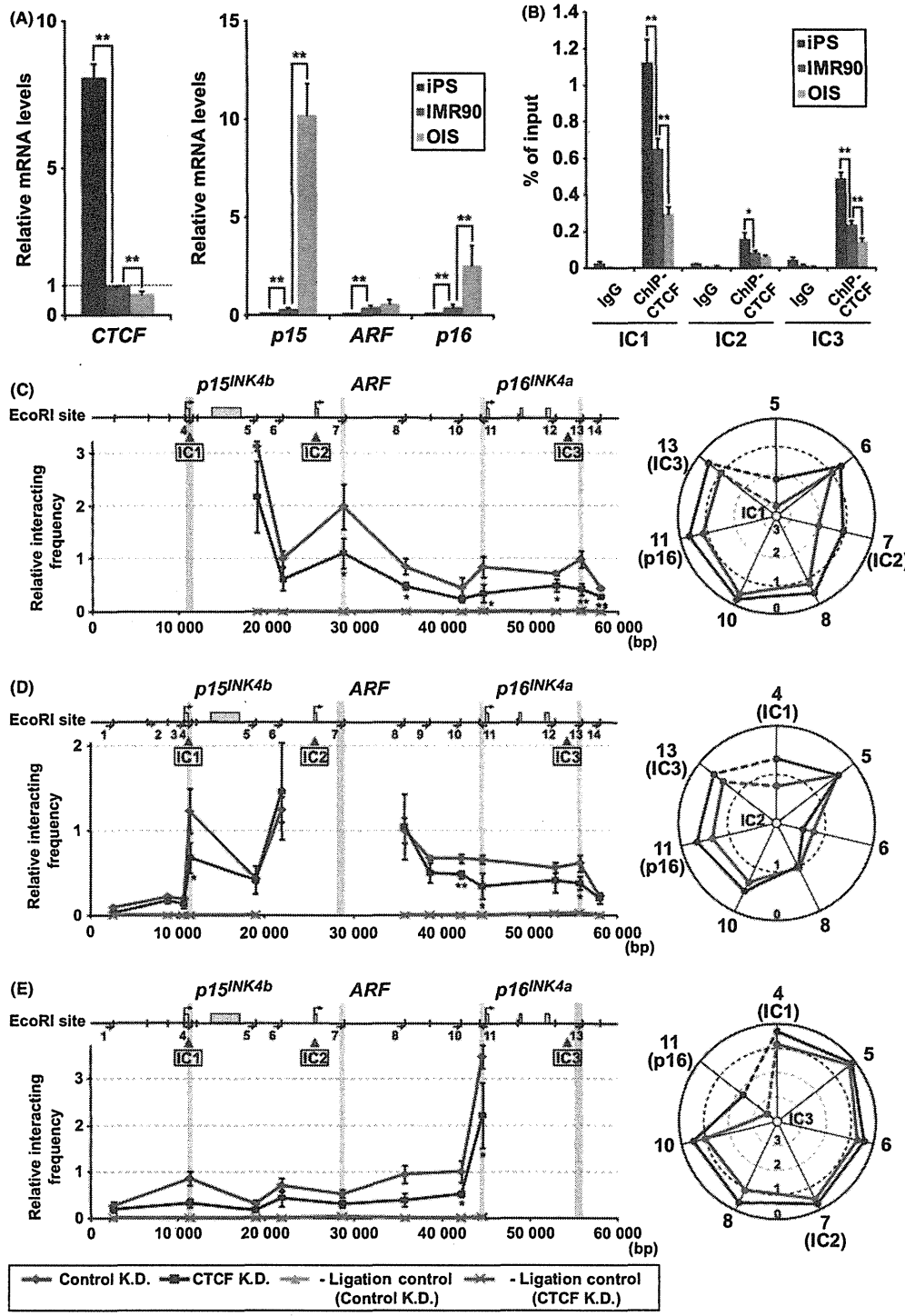

Fig. 1 CTCF is required for chromosomal conformation at the *INK4/ARF* locus. (A) Unique expression of *CTCF* and *INK4/ARF* genes. (B) Presence of CTCF at IC sites in human diploid fibroblasts (IMR90), Ras-induced senescent IMR90 cells (oncogene-induced senescent (OIS) cells), and 201B7 cells derived from human fibroblasts (iPS). CTCF-enriched sites (IC1, IC2 and IC3) are shown in Fig. S3A (Supporting information). (C–E) The relative interacting frequency with the references IC1/$p15^{INK4b}$ (C), IC2/*ARF* (D), and IC3 (E) in control and CTCF knockdown IMR90 cells. In chromosome conformation capture (3C) assay, interaction frequencies between the reference and its physically close site were normalized to 1 [IC1-fragment 6 (C), IC2-fragment 8 (D) and IC3-fragment 10 (E)]. Samples without ligation after *Eco*RI digestion are shown as ligation minus. Primer in each fragment is indicated by small arrow. In the right panel, the radar chart shows the average relative interacting frequencies between the reference (central yellow circle) and each fragment. Values are the means and standard deviations from more than three independent experiments. $*P < 0.05$, $**P < 0.01$.

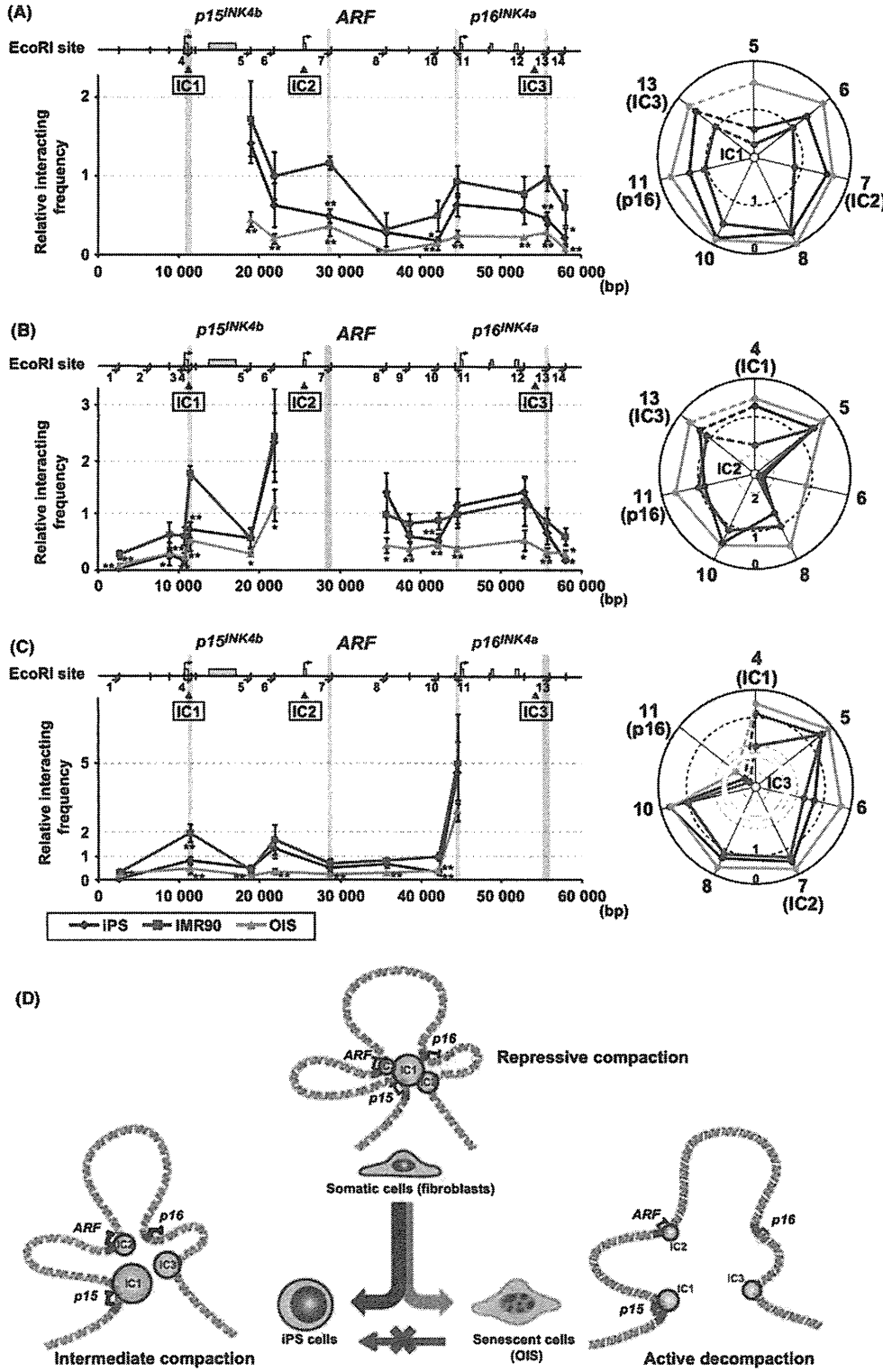

Fig. 2 Higher-order chromatin structure of the *INK4/ARF* locus in reprogrammed cells. (A–C) As described in Fig. 1, 3C analysis was performed in iPS, IMR90, and oncogene-induced senescent cells. (D) Somatic fibroblasts show compact chromatin loops for coordinate repression of *INK4/ARF* genes (repressive compaction), while senescent cells reduce CTCF binding and lose higher-order chromatin structure leading to activation of $p15^{INK4b}$ and $p16^{INK4a}$ (active decompaction). In iPS cells, the silenced *INK4/ARF* locus has moderately compact chromatin (intermediate compaction).

moter closely associated to form compact chromatin in IMR90 cells (red line). However, in OIS cells (green line), interaction frequencies of these references with other sites were remarkably reduced, paralleling CTCF binding decreases at IC1 and IC3 sites, compared with those in IMR90 cells. This suggests that the loose chromatin structure of the *INK4/ARF* locus occurred in OIS cells with *INK4* up-regulation. In iPS cells (blue line), interactions between IC sites also decreased to some extent. The interactions of the IC2/*ARF* with $p16^{INK4a}$ promoter and IC3 were retained in iPS cells, suggesting that the *INK4/ARF* locus in iPS cells has an intermediate state of chromatin compaction.

We demonstrated that CTCF is crucial for higher-order chromatin organization in the *INK4/ARF* locus in reprogrammed cells. As shown in Fig. 2D, we proposed the CTCF-mediated chromatin conformation model of the *INK4/ARF* locus: repressive compaction in growing fibroblasts, active decompaction in OIS cells, and intermediate compaction in iPS cells. Especially, OIS cells show a unique chromatin decompaction in the *INK4/ARF* locus, with marked induction of the *INK4* genes and senescence-associated nuclear changes (Figs S5 and S6, Supporting information), which may be a barrier for reprogramming to iPS cells. Our study uncovers that the higher-order chromatin signature provides the identity of senescent cells.

Acknowledgments

We would like to thank Dr. Hiroyuki Aburatani (University of Tokyo) for previous collaboration. This work was supported by grants from the Ministry of Education, Culture, Sports, Science, and Technology of Japan, from the Japan Science and Technology Agency (CREST), and from the Naito Foundation (M.N.).

References

Banito A, Rashid ST, Acosta JC, Li S, Pereira CF, Geti I, Pinho S, Silva JC, Azuara V, Walsh M, Vallier L, Gil J (2009) Senescence impairs successful reprogramming to pluripotent stem cells. *Genes Dev.* **23**, 2134–2139.

Collado M, Blasco MA, Serrano M (2007) Cellular senescence in cancer and aging. *Cell* **130**, 223–233.

Gil J, Peters G (2006) Regulation of the INK4b-ARF-INK4a tumour suppressor locus: all for one or one for all. *Nat. Rev. Mol. Cell Biol.* **7**, 667–677.

Kim WY, Sharpless NE (2006) The regulation of INK4/ARF in cancer and aging. *Cell* **127**, 265–275.

Li H, Collado M, Villasante A, Strati K, Ortega S, Canamero M, Blasco MA, Serrano M (2009) The Ink4/Arf locus is a barrier for iPS cell reprogramming. *Nature* **460**, 1136–1139.

Mishiro T, Ishihara K, Hino S, Tsutsumi S, Aburatani H, Shirahige K, Kinoshita Y, Nakao M (2009) Architectural roles of multiple chromatin insulators at the human apolipoprotein gene cluster. *EMBO J.* **28**, 1234–1245.

Narita M, Nunez S, Heard E, Lin AW, Hearn SA, Spector DL, Hannon GJ, Lowe SW (2003) Rb-mediated heterochromatin formation and silencing of E2F target genes during cellular senescence. *Cell* **113**, 703–716.

Ohlsson R, Lobanenkov V, Klenova E (2010) Does CTCF mediate between nuclear organization and gene expression? *BioEssays* **32**, 37–50.

Phillips JE, Corces VG (2009) CTCF: master weaver of the genome. *Cell* **137**, 1194–1211.

Serrano M, Lin AW, McCurrach ME, Beach D, Lowe SW (1997) Oncogenic ras provokes premature cell senescence associated with accumulation of p53 and p16INK4a. *Cell* **88**, 593–602.

Takahashi K, Tanabe K, Ohnuki M, Narita M, Ichisaka T, Tomoda K, Yamanaka S (2007) Induction of pluripotent stem cells from adult human fibroblasts by defined factors. *Cell* **131**, 861–872.

Wendt KS, Yoshida K, Itoh T, Bando M, Koch B, Schirghuber E, Tsutsumi S, Nagae G, Ishihara K, Mishiro T, Yahata K, Imamoto F, Aburatani H, Nakao M, Imamoto N, Maeshima K, Shirahige K, Peters JM (2008) Cohesin mediates transcriptional insulation by CCCTC-binding factor. *Nature* **451**, 796–801.

Supporting Information

Additional supporting information may be found in the online version of this article:

Fig. S1 Characteristics of reprogrammed human cell.

Fig. S2 Unique expression of *CTCF* and *INK4/ARF* genes in reprogrammed cells.

Fig. S3 Distribution of CTCF-enriched site at the *INK4/ARF* locus in cultured human cells.

Fig. S4 CTCF is involved in transcriptional control of the *INK4/ARF* locus.

Fig. S5 Histone modifications at the *INK4/ARF* locus in reprogrammed cells.

Fig. S6 Subnuclear localization of CTCF in somatic and reprogrammed cells.

Table S1 The list of primer sets.

As a service to our authors and readers, this journal provides supporting information supplied by the authors. Such materials are peer-reviewed and may be re-organized for online delivery, but are not copy-edited or typeset. Technical support issues arising from supporting information (other than missing files) should be addressed to the authors.

Case Reports in Gastroenterology

Case Rep Gastroenterol 2012;6:590–595
DOI: 10.1159/000343157

Published online: September 18, 2012

ISSN 1662–0631
www.karger.com/crg

Primary Hepatic Gastrinoma as an Unusual Manifestation of Zollinger-Ellison Syndrome

Hideaki Naoe[a] Hajime Iwasaki[a] Takeshi Kawasaki[a]
Tetsu Ozaki[a] Hideharu Tsutsumi[a] Ayako Okuda[a]
Takeyasu Konoe[a] Kouichi Nonaka[a] Eisuke Kaku[a]
Takashi Shono[a] Kazunori Yokomine[a] Kouichi Sakurai[a]
Ken-ichi Iyama[b] Masahiko Hirota[c] Yutaka Sasaki[a]

Departments of [a]Gastroenterology and Hepatology and [b]Surgical Pathology, Graduate School of Medical Sciences, Kumamoto University, and [c]Department of Surgery, Kumamoto Regional Medical Center, Kumamoto, Japan

Key Words
Gastrinoma · Zollinger-Ellison syndrome · Arterial stimulation and venous sampling test

Abstract
We report a rare case of primary hepatic gastrinoma. A 77-year-old woman exhibited continuous watery diarrhea for 8 months and weight loss. Bacterial cultures of the stools were negative and colonoscopy revealed no abnormalities. Esophagogastroduodenoscopy showed severe reflux esophagitis and multiple duodenal erosions. Computed tomography and magnetic resonance imaging detected two solid masses measuring <2 cm in diameter in the right lobe of the non-cirrhotic liver. Microscopically, the tumor was consistent with neuroendocrine tumor (grade 2) with abundant gastrin-immunoreactive cells. Endoscopic ultrasound detected no other alternative primary source of an endocrine tumor. The serum gastrin levels exceeded 40,000 pg/ml in the absence of H_2 receptor antagonist and proton pump inhibitor administrations. Based on an arterial stimulation and venous sampling test, the patient was diagnosed as primary gastrinoma of the liver. Our findings demonstrated the presence of Zollinger-Ellison syndrome in a patient who was subsequently cured by surgical resection of the liver tumors.

Yutaka Sasaki

Department of Gastroenterology and Hepatology
Graduate School of Medical Sciences, Kumamoto University
Kumamoto 860-8556 (Japan)
E-Mail sasakiy@kumamoto-u.ac.jp

Case Rep Gastroenterol 2012;6:590–595
DOI: 10.1159/000343157
Published online: September 18, 2012

ISSN 1662–0631
www.karger.com/crg

Introduction

Gastrinoma-induced Zollinger-Ellison syndrome (ZES) is characterized by refractory peptic ulcers of the upper gastrointestinal tract, diarrhea and gastric acid hypersecretion associated with non-beta islet cell tumors of the pancreas [1]. Most reports suggest that the diagnosis of ZES can be established in patients with gastrin levels >1,000 pg/ml or 10-fold higher than standard level, associated with acid production [1–4].

More than half of all gastrinomas are sporadic, whereas approximately 18–25% are associated with multiple endocrine neoplasia type 1 (MEN-1) syndrome, which is characterized by pancreatic endocrine tumors, pituitary adenomas and parathyroid hyperplasia [1, 2, 5]. At the time of diagnosis, 50–60% of gastrinomas are malignant and associated with metastases [2]. The only way to cure patients without non-resectable metastatic disease is to perform surgery.

Gastrinomas are frequently small in size and are often difficult to find preoperatively. Selective arterial secretin or calcium stimulation with sampling from the hepatic veins is helpful for detecting the localization of gastrinomas. In this test, the diagnosis is established if a more than two-fold increase in gastrin concentration is observed in the hepatic vein after secretin/calcium injection.

Recent progress has cultivated our understanding of the molecular bases of gastrinoma. Indeed, alterations in several oncogenes including c-Myc, HER2/neu (ElbB-2) and tumor suppressor genes such as MEN-1 and P16 (INK4a) have been reported [1]. In addition, mutations in biologic factor such as growth factors and receptors have been described. However, these alterations are not absolutely correlated with aggressive biology [1]. More precise mechanisms, therefore, need to be clarified with regard to tumorigenesis of gastrinoma.

The vast majority of gastrinomas are found in the pancreas or duodenum [3, 6, 7]. Although sporadic gastrinomas not associated with MEN-1 have been reported in other locations, including the liver, these ectopic gastrinomas are rare [1, 7]. To the best of our knowledge, less than 30 cases of primary hepatic gastrinomas have been reported in the literature [3, 7]. In this report, we present a patient with two small primary gastrinomas in the liver, who was cured by surgical resection of the tumors. The unique feature of our case is that there were two independent small tumors in the liver, both of which were diagnosed as gastrinoma pathologically.

Case Report

A 77-year-old woman was admitted to our hospital with chief complaints of diarrhea for 8 months and a weight loss of 6 kg. Diarrhea without blood was seen 7–10 times a day. Bacterial cultures of the stools were repeatedly negative. Colonoscopy revealed no significant abnormalities. Esophagogastroduodenoscopy showed severe erosive esophagitis (fig. 1a), erosive gastritis, and multiple ulcers that were accompanied by surrounding edema in the second portion of the duodenum (fig. 1b). Ultrasonography showed that the patient had two small hypoechoic lesions in the right lobe of the liver. A plain computed tomography (CT) scan showed two low-attenuation round lesions in the right hepatic lobe (fig. 2a). A contrast-enhanced CT scan obtained during the arterial phase demonstrated a 19 mm ring enhancing mass (fig. 2b, arrow) with washout in the delayed phase (fig. 2c, arrow) in the subcapsular lesion of the right hepatic lobe, and a 16 mm faintly enhancing mass (fig. 2d, arrowhead)

Case Rep Gastroenterol 2012;6:590–595
DOI: 10.1159/000343157
Published online: September 18, 2012

ISSN 1662–0631
www.karger.com/crg

with washout in the delayed phase (fig. 2e, arrowhead) within the posterior segment of the right hepatic lobe. Magnetic resonance imaging (MRI) confirmed the CT findings of masses in the liver and additionally showed a normal pancreas and no evidence of tumors at any other sites (fig. 2f). Endoscopic ultrasound also revealed no tumors in the pancreas and the duodenal wall (data not shown). Transcutaneous tumor biopsy can be used to identify the type of liver tumor that is present. Our pathological examination found there was a solid growth of uniform middle-sized neuroendocrine tumor cells (grade 2) with eosinophilic granules (fig. 3a). Immunohistochemically, the tumor cells were positive for gastrin (fig. 3a, inset) and negative for insulin, VIP, glucagon, somatostatin and somatostatin receptors (data not shown). The MIB-1 labeling index of this tumor was approximately 20% (fig. 3b). The serum gastrin level was checked upon admission and determined to be 41,000 pg/ml.

As the patient was not receiving any acid-suppressive medication when first examined, we initially suspected the presence of gastrinoma in the duodenum or pancreas, with metastasis to the liver. However, since there was no evidence of gastrinoma in the pancreas or the duodenal wall, we attempted to detect the site of the gastrinoma by using arterial stimulation and venous sampling (ASVS) tests. Proper hepatic artery, dorsal pancreatic artery, gastroduodenal artery, splenic artery and superior mesenteric artery were selectively catheterized for stimulation by rapid injection of calcium gluconate. Blood was sampled through the hepatic vein before as well as 30, 60, 90, 120 and 180 s after calcium gluconate injection. All hepatic vein samples showed equally high gastrin levels (table 1). These results suggested that the primary gastrinoma might be the two small tumors that were observed in the liver.

To exclude MEN-1, brain MRI and thyroid ultrasonography was performed. However, no apparent abnormalities were detected in either the pituitary or the parathyroid glands. In addition, FDG PET showed no abnormal uptake in the liver or at any other site. Finally, a right lateral segmentectomy of the liver was performed to remove the liver tumors. In line with our preoperative diagnosis, the pathological examination revealed two gastrinomas in the right lobe of the liver.

Twelve months after the operation, the patient remains asymptomatic and her serum gastrin levels are within the normal range. These findings are consistent with a surgical cure of ZES.

Discussion

In 1955, Zollinger and Ellison described a syndrome characterized by ulceration of the upper jejunum, hypersecretion of gastric acid and non-beta islet cell tumors of the pancreas [8]. Similar to that seen in our current case, diarrhea has been shown to be one of the most common symptoms, with its presence documented in >70% of patients. Gastric acid hypersecretion may cause direct intestinal mucosal injury and inactivation of pancreatic enzymes, which results in diarrhea [7]. Additionally, patients rarely present with only one symptom. While weight loss with abdominal pain and diarrhea are important symptoms that suggest the presence of gastrinoma, it is difficult to diagnose ZES initially, as the mean delay from onset to diagnosis has been reported to be 5–6 years [1, 6, 9]. Of 261 ZES patients treated at the National Institutes of Health, 98% were misdiagnosed prior to establishing a final diagnosis of ZES [9]. Unfortunately, the diagnosis of ZES is becoming more difficult due to the widespread use of proton pump inhibitors (PPIs) as the symptoms can be masked by long-term treatment with PPIs [1]. In fact, it was shown that when patients were being treated with either PPIs or H_2 receptor antagonists, it was not possible to make a gastrinoma diagnosis based on the fasting plasma gastrin levels [2].

In contrast, selective arterial secretin or calcium stimulation with sampling from the hepatic veins is helpful in detecting the localization of the gastrinoma [4, 10]. Since these compounds stimulate the release of gastrin by the gastrinoma tumor cells,

Case Rep Gastroenterol 2012;6:590–595
DOI: 10.1159/000343157
Published online: September 18, 2012

ISSN 1662–0631
www.karger.com/crg

patients with gastrinomas show a rapid rise in the serum gastrin level in response to the administration of secretin or calcium [1]. When we performed an ASVS test for the current case, we were unable to detect any significant changes in the serum gastrin levels, with the gastrin levels of all samples taken from the hepatic vein found to be equally extremely high. Thus, these observations suggested that the gastrinoma was potentially located in the liver. It has been previously shown that gastrinomas arise in the so-called 'gastrinoma triangle', which is defined by the junction of the cystic duct and common bile duct, the junction of the second and third portions of the duodenum, and the junction between the neck and body of the pancreas [1, 2].

However, ectopic gastrinomas that occur outside of the gastrinoma triangle are rare, with <30 primary hepatic gastrinomas having been reported in the literature [3, 7]. In the NIH study, primary hepatic gastrinomas occurred in <2% of the ZES patients [9]. Although most gastrinomas grow slowly, 60–90% of these gastrinomas are malignant, with 25% showing rapid growth [1, 2, 5]. Therefore, the only way to cure these patients is to perform surgery, which needs to be considered in all patients without MEN-1, provided the tumor is resectable.

In conclusion, we report a rare case of primary hepatic gastrinoma. Evaluation of the patient using preoperative image diagnosis and an ASVS test led to surgical excision of the tumors and cure of the patient.

Table 1. Serum gastrin levels (pg/ml) before and after calcium injection

Calcium injection site	Time, min					
	0	30	60	90	120	180
PHA	36,000	41,000	40,000	37,000	39,000	40,000
DPA	45,000	43,000	39,000	46,000	41,000	44,000
GDA	45,000	49,000	41,000	42,000	45,000	46,000
SA	46,000	39,000	40,000	42,000	41,000	39,000
SMA	41,000	38,000	39,000	39,000	38,000	38,000

Gastrin concentrations were measured in the hepatic vein after calcium gluconate injection directly into the respective arteries. PHA = Proper hepatic artery; DPA = dorsal pancreatic artery; GDA = gastroduodenal artery; SA = splenic artery; SMA = superior mesenteric artery.

Case Rep Gastroenterol 2012;6:590–595
DOI: 10.1159/000343157
Published online: September 18, 2012

ISSN 1662–0631
www.karger.com/crg

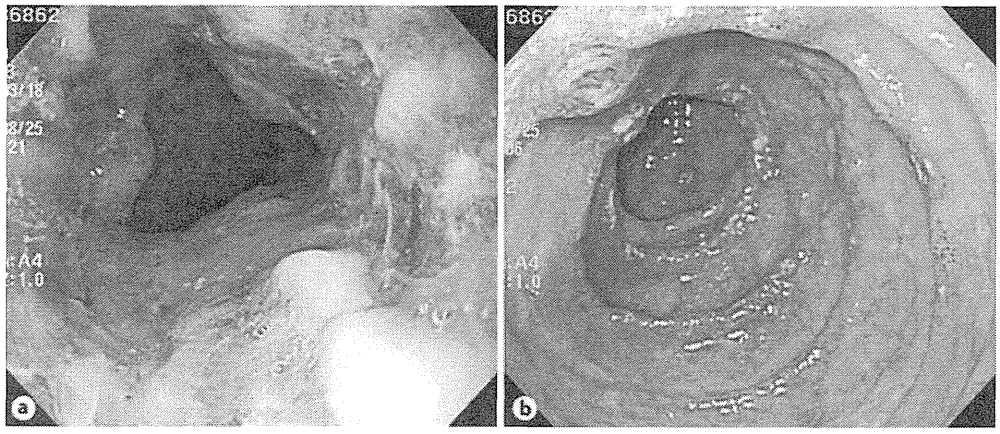

Fig. 1. Esophagogastroduodenoscopy showing severe erosive esophagitis and duodenitis. **a** Circumferential reflux esophagitis with superficial ulceration was observed in the distal esophagus near the gastroesophageal junction. **b** Multiple erosions with surrounding edema were found in the second portion of the duodenum.

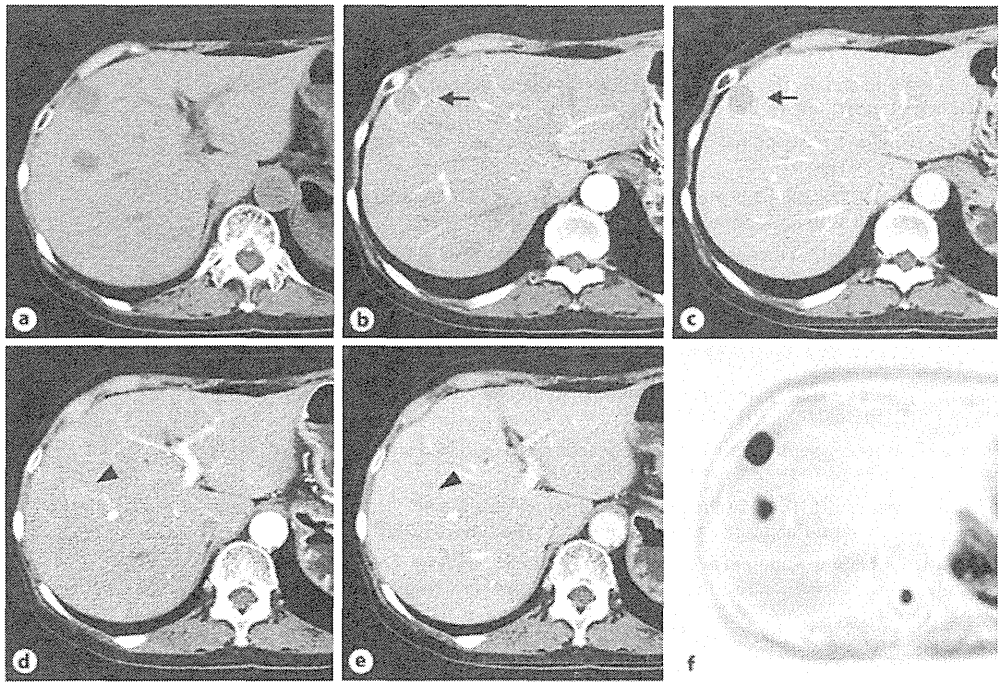

Fig. 2. Diagnostic imaging showing two masses in the right hepatic lobe. **a** A plain CT scan of the abdomen revealed two low-attenuation round lesions in the right hepatic lobe. A contrast-enhanced CT scan showed a 19 mm ring enhancement (**b**, arrow) in the arterial phase with washout in the delayed phase (**c**, arrow) within the subcapsular lesion. A 16 mm faintly enhancing mass (**d**, arrowhead) in the arterial phase with washout in the delayed phase (**e**, arrowhead) was seen within the posterior segment of the right hepatic lobe. The high signals seen for the tumors on the diffusion-weighted MR image are consistent with diffusion restriction (**f**).

Case Rep Gastroenterol 2012;6:590–595
DOI: 10.1159/000343157
Published online: September 18, 2012

ISSN 1662–0631
www.karger.com/crg

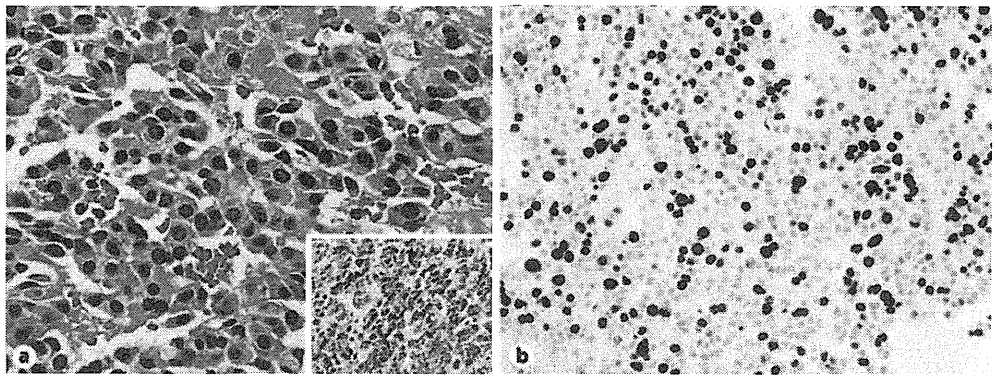

Fig. 3. Pathological and immunohistochemical findings consistent with gastrinoma. **a** Pathological findings showed a neuroendocrine tumor consistent with gastrinoma. Stains are positive for gastrin (inset). **b** MIB-1 labeling index of this tumor was approximately 20%.

References

1 Ellison EC, Johnson JA: The Zollinger-Ellison syndrome: a comprehensive review of historical, scientific, and clinical considerations. Curr Probl Surg 2009;46:13–106.

2 Fendrich V, Langer P, Waldmann J, Bartsch DK, Rothmund M: Management of sporadic and multiple endocrine neoplasia type 1 gastrinomas. Br J Surg 2007;94:1331–1341.

3 Ito T, Jensen RT: Primary hepatic gastrinoma: an unusual case of Zollinger-Ellison syndrome. Gastroenterol Hepatol (N Y) 2010;6:57–59.

4 Turner JJ, Wren AM, Jackson JE, Thakker RV, Meeran K: Localization of gastrinomas by selective intra-arterial calcium injection. Clin Endocrinol (Oxf) 2002;57:821–825.

5 Norton JA, Fraker DL, Alexander HR, Venzon DJ, Doppman JL, Serrano J, Goebel SU, Peghini PL, Roy PK, Gibril F, Jensen RT: Surgery to cure the Zollinger-Ellison syndrome. N Engl J Med 1999;341:635–644.

6 Wu PC, Alexander HR, Bartlett DL, Doppman JL, Fraker DL, Norton JA, Gibril F, Fogt F, Jensen RT: A prospective analysis of the frequency, location, and curability of ectopic (nonpancreaticoduodenal, nonnodal) gastrinoma. Surgery 1997;122:1176–1182.

7 Evans JT, Nickles S, Hoffman BJ: Primary hepatic gastrinoma: an unusual case of Zollinger-Ellison syndrome. Gastroenterol Hepatol (N Y) 2010;6:53–56.

8 Zollinger RM, Ellison EH: Primary peptic ulcerations of the jejunum associated with islet cell tumors of the pancreas. Ann Surg 1955;142:709–723; discussion 724–728.

9 Roy PK, Venzon DJ, Shojamanesh H, Abou-Saif A, Peghini P, Doppman JL, Gibril F, Jensen RT: Zollinger-Ellison syndrome. Clinical presentation in 261 patients. Medicine (Baltimore) 2000;79:379–411.

10 Imamura M, Takahashi K, Adachi H, Minematsu S, Shimada Y, Naito M, Suzuki T, Tobe T, Azuma T: Usefulness of selective arterial secretin injection test for localization of gastrinoma in the Zollinger-Ellison syndrome. Ann Surg 1987;205:230–239.

Biochemical and Biophysical Research Communications 430 (2013) 757–762

Contents lists available at SciVerse ScienceDirect

Biochemical and Biophysical Research Communications

journal homepage: www.elsevier.com/locate/ybbrc

The APC/C activator Cdh1 regulates the G2/M transition during differentiation of placental trophoblast stem cells

Hideaki Naoe [a,b], Tatsuyuki Chiyoda [a], Jo Ishizawa [a,c], Kenta Masuda [a], Hideyuki Saya [a], Shinji Kuninaka [a,*]

[a] Division of Gene Regulation, Institute for Advanced Medical Research, Keio University School of Medicine, Tokyo 160-8582, Japan
[b] Department of Gastroenterology and Hepatology, Kumamoto University, School of Medicine, Kumamoto 860-8556, Japan
[c] Division of Hematology, Department of Medicine, Keio University School of Medicine, Tokyo 160-8582, Japan

ARTICLE INFO

Article history:
Received 7 November 2012
Available online 1 December 2012

Keywords:
Cdh1
APC/C
Endocycle
G2/M transition
Trophoblast stem cell
Trophoblast giant cell

ABSTRACT

Differentiation of placental trophoblast stem (TS) cells to trophoblast giant (TG) cells is accompanied by transition from a mitotic cell cycle to an endocycle. Here, we report that Cdh1, a regulator of the anaphase-promoting complex/cyclosome (APC/C), negatively regulates mitotic entry upon the mitotic/endocycle transition. TS cells derived from homozygous *Cdh1* gene-trapped ($Cdh1^{GT/GT}$) murine embryos accumulated mitotic cyclins and precociously entered mitosis after induction of TS cell differentiation, indicating that Cdh1 is required for the switch from mitosis to the endocycle. Furthermore, the $Cdh1^{GT/GT}$ TS cells and placenta showed aberrant expression of placental differentiation markers. These data highlight an important role of Cdh1 in the G2/M transition during placental differentiation.

1. Introduction

The endocycle, also known as the endoreplicative cycle, is a well-conserved process that occurs in both plants and animals. This specific type of cell cycle is mechanistically unusual in that it bypasses several controls that are fundamental to the regulation of the mitotic cycle [1]. During the endocycle, cells undergo repeated rounds of DNA replication without completing cell division, leading to polyploidy [2].

A good example of the endocycle can be seen in *Drosophila*. *Drosophila* follicle cells, which comprise the egg chamber, divide mitotically until mid-oogenesis and then uniformly exit the mitotic cycle to enter the endocycle thereafter [3]. When a cell transits from the mitotic cycle to the endocycle, the block of mitotic entry is an essential step. Cdh1 (also known as Fzr) activates the anaphase-promoting complex/cyclosome (APC/C) to inhibit entry into mitosis via destruction of mitotic cyclins. Cells of Cdh1 loss-of-function fly mutants are unable to enter the endocycle [4,5].

In contrast to *Drosophila*, the endocycle in mammals is infrequent. Such rare cases can be seen in the rodent placenta, where differentiation of trophoblast stem (TS) cells to trophoblast giant (TG) cells is contingent upon the endocycle. A recent study indicated that the cyclin-dependent kinase (Cdk) inhibitor p57 inhibits mitotic entry for endocycle initiation in TS cells [6]. Following FGF4 deprivation to induce differentiation, most, but not all, $p57^{-/-}$ TS cells are unable to increase DNA content to more than 4 N [6]. However, the DNA content in placental TG cells of *p57* homozygous knockout mice is not significantly reduced compared to wild-type TG cells [7,8], suggesting that a p57-independent regulator of the mitotic/endocycle switch exists in mammals.

Several groups have generated Cdh1 deficient mice and found that their placental TG cells show significantly reduced ploidy compared with their wild-type counterparts [9–11], indicating the involvement of Cdh1 in the mammalian endocycle, as in *Drosophila*. Nonetheless, it is unclear how Cdh1 regulates the endocycle in TS cells. To clarify this issue, we established *Cdh1* gene-trap (GT) TS cells and examined the role of Cdh1 in the regulation of mitotic entry at the mitotic/endocycle transition.

2. Materials and methods

2.1. Cdh1 gene-trap mice

$Cdh1^{+/GT}$ mice (C57BL/6 background) were established and maintained as described previously [11]. All animal experiments were approved by the Animal Ethics Committee of Keio University.

Abbreviations: APC/C, anaphase-promoting complex/cyclosome; TS cell, trophoblast stem cell; TG cell, trophoblast giant cell; GT, gene-trap; F4H, FGF4 and heparin; CM, conditioned medium.

* Corresponding author. Address: Division of Gene Regulation, Institute for Advanced Medical Research, Keio University School of Medicine, 35 Shinanomachi, Shinjuku-ku, Tokyo 160-8582, Japan. Fax: +81 3 5363 3982.
E-mail address: skuninak@a8.keio.jp (S. Kuninaka).

0006-291X/$ - see front matter © 2012 Elsevier Inc. All rights reserved.
http://dx.doi.org/10.1016/j.bbrc.2012.11.075

2.2. Isolation and maintenance of TS cells

TS cells were derived from E3.5 blastocysts and were established and cultured as described previously [12,13]. In brief, after mating with $Cdh1^{+/GT}$ male mice, a pregnant female $Cdh1^{+/GT}$ mouse was sacrificed at 3.5 dpc and the uterus was removed. Blastocysts were flushed out of the uterus with M2 medium (Sigma) using a 26 gauge needle. Each blastocyst was cultured on feeder cells in TS medium (RPMI-1640 (Sigma) supplemented with 20% fetal calf serum (Nichirei, Tokyo, Japan), 100 μM 2-mercaptoethanol (Invitrogen), 1 mM sodium pyruvate (Invitrogen), 1× antibiotic–antimycotic (Invitrogen), and 1×F4H (25 μg/ml FGF-4 (Peprotech) and 1 μg/ml Heparin (Sigma)). When the outgrowths reached a visible size, cells were trypsinized to dissociate and transferred to colony formation cultures. TS colonies were cultured on feeder cells in 70 CM (7:3 mixture of TS medium conditioned by mouse embryonic fibroblasts (MEFs) and fresh TS medium) containing 1.5×F4H until appropriate cell densities were attained, and colonies were then maintained in TS medium containing 1×F4H. For feeder-free cultures, TS cells were maintained in gelatin-coated dishes in 70 CM containing 1×F4H.

2.3. Immunocytochemistry

Immunofluorescence staining was performed as described previously [14] using antibodies to E-cadherin (1:500 dilution; BD), or Ser^{10}-phosphorylated histone H3 (1:100 dilution; Cell Signaling). Sections were observed with a Fluoview laser-scanning confocal microscope (IX70, Olympus) equipped with a 60× objective (numerical aperture, 1.25). The size of the nuclei (represented by the number of pixels) in Hoechst 33342-stained cells was determined using the ImageXpress and Metamorph software (Molecular Devices).

2.4. Western blotting

TS cells were cultured in the absence of F4H and collected at the indicated times after F4H deprivation. Cells were washed in phosphate buffered saline and lysed by incubation for 15 min in lysis buffer (0.5% NP-40, 25 mM Tris–Cl (pH 7.5), 150 mM NaCl, 1 mM $MgCl_2$, 10% glycerol, and complete protease inhibitor cocktail (EDTA free; Roche)). After centrifugation of the lysates at 14,000*g* for 20 min, the supernatant was subjected to SDS gel electrophoresis, Western blotting, and immunodetection using the indicated antibodies. Antibodies used in this study were as follows: Cyclin B (GNS1, Santa Cruz), Cyclin A (C-19, Santa Cruz), Cdh1 (DH01, Neomarkers), Cdc20 (H7, Santa Cruz), Skp2 (GP45, Zymed), Aurora A (clone4, BD), p27 (C-19, Santa Cruz), p57 (E-17, Santa Cruz), α-tubulin (B5-1-2, Sigma), PL-1 (AB1288, Chemicon) and Cdk4 (Ab-2, Neomarkers).

2.5. In situ hybridization

In situ hybridization was performed on sections of staged placentas as described previously [15], with some modifications in the signal detection by using a DIG-labeled RNA probe (Roche). All plasmids used for the preparation of riboprobes were kindly provided by G. Leone [16]. Digoxigenin-UTP-labeled antisense and control (sense) riboprobes were synthesized from plasmids using SP6 or T7 RNA polymerase and the MAXIscript *in vitro* transcription kit (Ambion).

2.6. Quantitative analysis of gene expression

Total RNA was extracted from TS cells using an RNeasy Minikit (Qiagen) and was subjected to reverse transcription (RT) using PrimeScript (Takara). Real-time PCR was performed in a Thermal Cycler Dice apparatus (Takara) using SYBR Premix Ex Taq (Takara). All primers used to amplify trophoblast marker genes have been described previously [17]. Primers for the murine Cdh1 and glyceralehyde-3-phosphate dehydrogenase (GAPDH) genes were obtained from Takara. Relative mRNA levels were calculated by normalization of cycle threshold (C_t) values of the target gene to those of the reference genes (GAPDH and ubiquitin).

2.7. Flow cytometry

Asynchronously growing TS cells were stained with propidium iodide and collected using a FACSCalibur apparatus (BD) combined with the CellQuest software (BD). Cell-cycle profiles were analyzed using the FlowJo software (Version 7.2.5; Tree Star, Inc.).

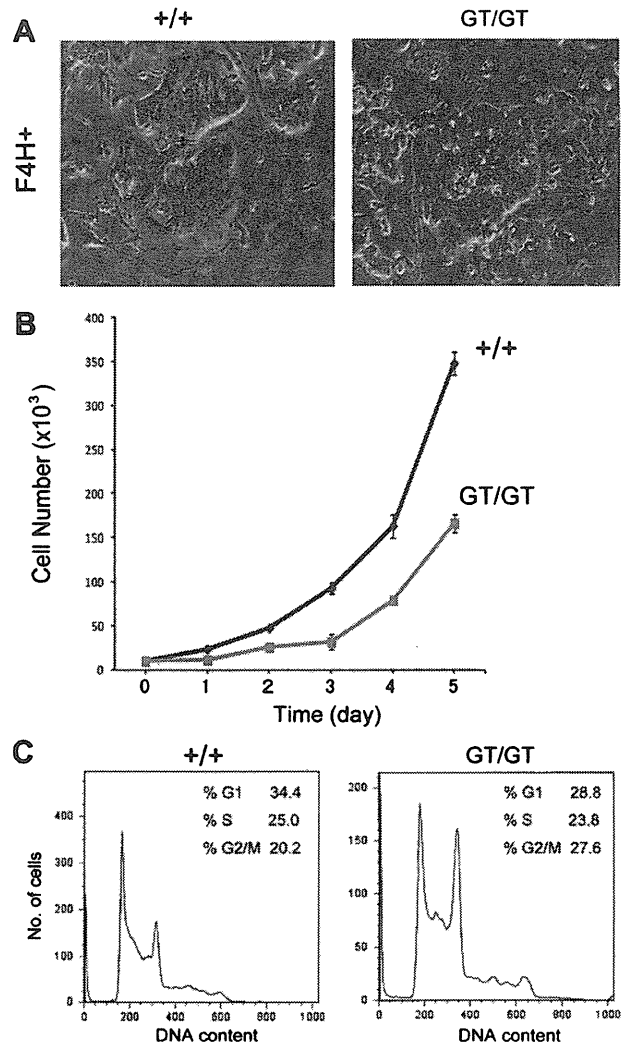

Fig. 1. Characterization of $Cdh1^{GT/GT}$ TS cells. (A) Establishment of $Cdh1^{GT/GT}$ TS cells. TS cells of the indicated *Cdh1* genotypes were cultured on feeder cells in the presence of FGF4/Heparin (F4H) (undifferentiated TS cells), and were then examined by phase-contrast microscopy. Original magnification, 40×. (B) Cell proliferation of undifferentiated TS cells with the indicated *Cdh1* genotypes was analyzed by seeding 1×10^5 cells in 70 CM medium containing F4H onto feeder-free dishes (gelatin-coated) and determining the cell number every 24 h. (C) Flow cytometric analysis of TS cells with the indicated *Cdh1* genotypes stained with propidium iodide. The fraction of cells in each stage of the cell cycle is presented.

2.8. Statistical analyses

Quantitative data are presented as means ± standard deviation (SD). Differences in nuclear size were determined by the Wilcoxon–Mann–Whitney nonparametric test using the JMP7 software (SAS Institute, Inc). Differences in the percentage of mitotic cells were evaluated using the two-tailed Student's *t* test. A value of $P < 0.05$ was considered significant.

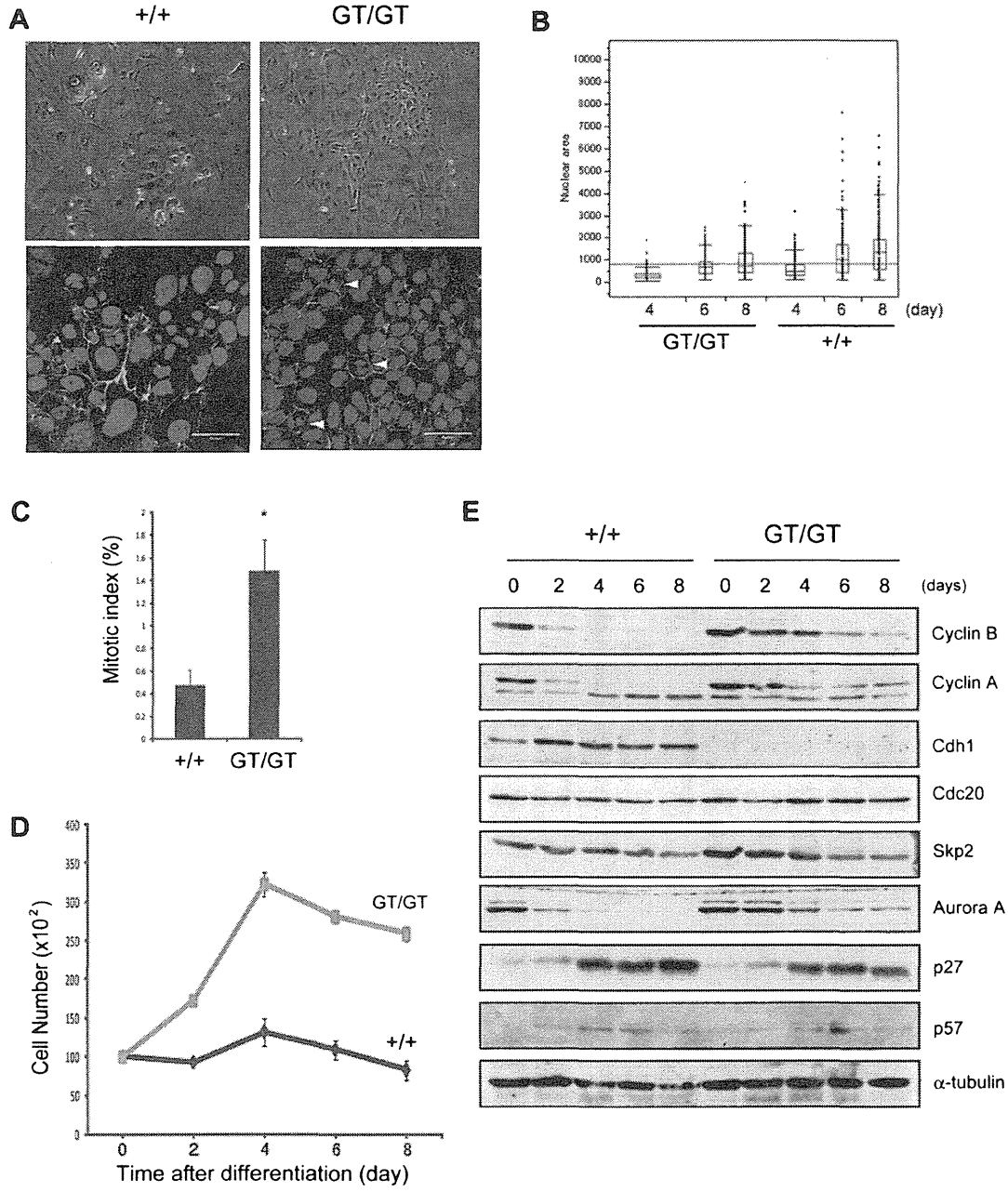

Fig. 2. Precocious mitotic entry and impaired endoreplication in *Cdh1*$^{GT/GT}$ TS cells after the induction of differentiation. (A) Loss of nuclear enlargement in *Cdh1*$^{GT/GT}$ TS cells. Upper panels: TS cells of the indicated *Cdh1* genotypes were cultured on feeder cells in the absence of F4H for 5 days and were then examined by phase-contrast microscopy (original magnification, 40×). Lower panels: TS cells cultured for 3 days in the absence of F4H were stained with propidium iodide (red) and antibodies to E-cadherin (green). Arrowheads indicate mitotic cells. Scale bars, 50 μm. (B) TS cells were cultured for the indicated times in the absence of F4H, and were then fixed and stained for DNA using Hoechst 33342. The size of over 200 nuclei (represented by the number of pixels on the *y* axis) was determined for each sample; bars on the dot plot denote the 10th and 90th percentiles, and each box indicates the first and third quartiles. The bar in each box shows the median value. Data are representative of two independent experiments. (C) The mitotic index of TS cells cultured for 5 days in the absence of F4H was measured by immunostaining with antibodies to phosphorylated histone H3. Data are means ± SD for over 800 cells scored for each genotype in two independent experiments. $^*P < 0.05$. (D) Growth curves for wild-type and *Cdh1*$^{GT/GT}$ TS cells after the induction of differentiation. Data are means ± SD from three independent experiments. (E) Immunoblot analysis of the indicated proteins in TS cells cultured in the absence of F4H for the indicated times after induction of differentiation. (For interpretation of the references to color in this figure legend, the reader is referred to the web version of this article.)

3. Results

3.1. Characterization of *Cdh1*$^{GT/GT}$ TS cells

Previous analysis of *Cdh1* homozygous GT (*Cdh1*$^{GT/GT}$) placentas revealed frequent thrombus formation in the labyrinth layer [11]. Another striking pathology in Cdh1-deficient placentas is a lack of giant nuclei in TG cells. The TG cells also contained significantly fewer genome copies (N) than their wild-type counterparts (wild-type, 100–1500 N; Cdh1$^{-/-}$, <100 N) [9,11].

To elucidate the molecular mechanisms by which Cdh1 regulates the endocycle in TG cells, we established *Cdh1*$^{GT/GT}$ TS cells from E3.5 blastocysts, as previously described [12]. TS cells have the potential to give rise to all differentiated trophoblast cell subtypes, including TG cells, and to reconstitute the placenta in chimeric animals [12]. Both wild-type and *Cdh1*$^{GT/GT}$ TS cells manifested a similar epithelial sheet morphology when cultured in TS medium supplemented with a combination of fibroblast growth factor 4 and heparin (F4H) (Fig. 1A). The proliferative capacity of undifferentiated TS cells was examined. *Cdh1*$^{GT/GT}$ TS cells proliferated at a slower rate when compared with wild-type TS cells (Fig. 1B), indicating that Cdh1 is required for TS cell division, as previously shown in MEFs [9,10]. Flow cytometric analysis of the cell-cycle profile of TS cells revealed that Cdh1 ablation resulted in an increase in the proportion of cells in the G2/M phase and a decrease in the fraction of cells in the G1 phase (Fig. 1C), a phenotype similar to that of Cdh1-deficient MEFs, with the exception of S phase. Only a minor decrease in the number of S phase *Cdh1*$^{GT/GT}$ TS cells compared to wild-type cells was detected [9,18] (Fig. 1C).

3.2. Precocious mitotic entry of *Cdh1*$^{GT/GT}$ TS cells after endocycle induction

Whether the *Cdh1*$^{GT/GT}$ TS cells recapitulate the pathological changes seen in *Cdh1*$^{GT/GT}$ placentas was examined next. In the absence of F4H, wild-type TS cells ceased to proliferate as a part of the mitotic/endocycle switch and differentiated into cells with giant nuclei (Fig. 2A and D). By contrast, the ability of *Cdh1*$^{GT/GT}$ TS cells to form structures with giant nuclei was markedly impaired (Fig. 2A). To evaluate the extent of polyploidy after various times in culture in the absence of F4H, the area occupied by the nuclei in these cells was measured (Fig. 2B). The ploidy of *Cdh1*$^{GT/GT}$ TG cells was significantly reduced compared with that of wild-type cells ($P < 0.0001$), indicating that Cdh1 plays an important role in the mammalian endocycle and that our *in vitro* system closely resembles the *in vivo* situation [9,11].

Upon the mitotic/endocycle switch, mitotic entry is inhibited in wild-type TS cells. However, mitotic cells were frequently observed

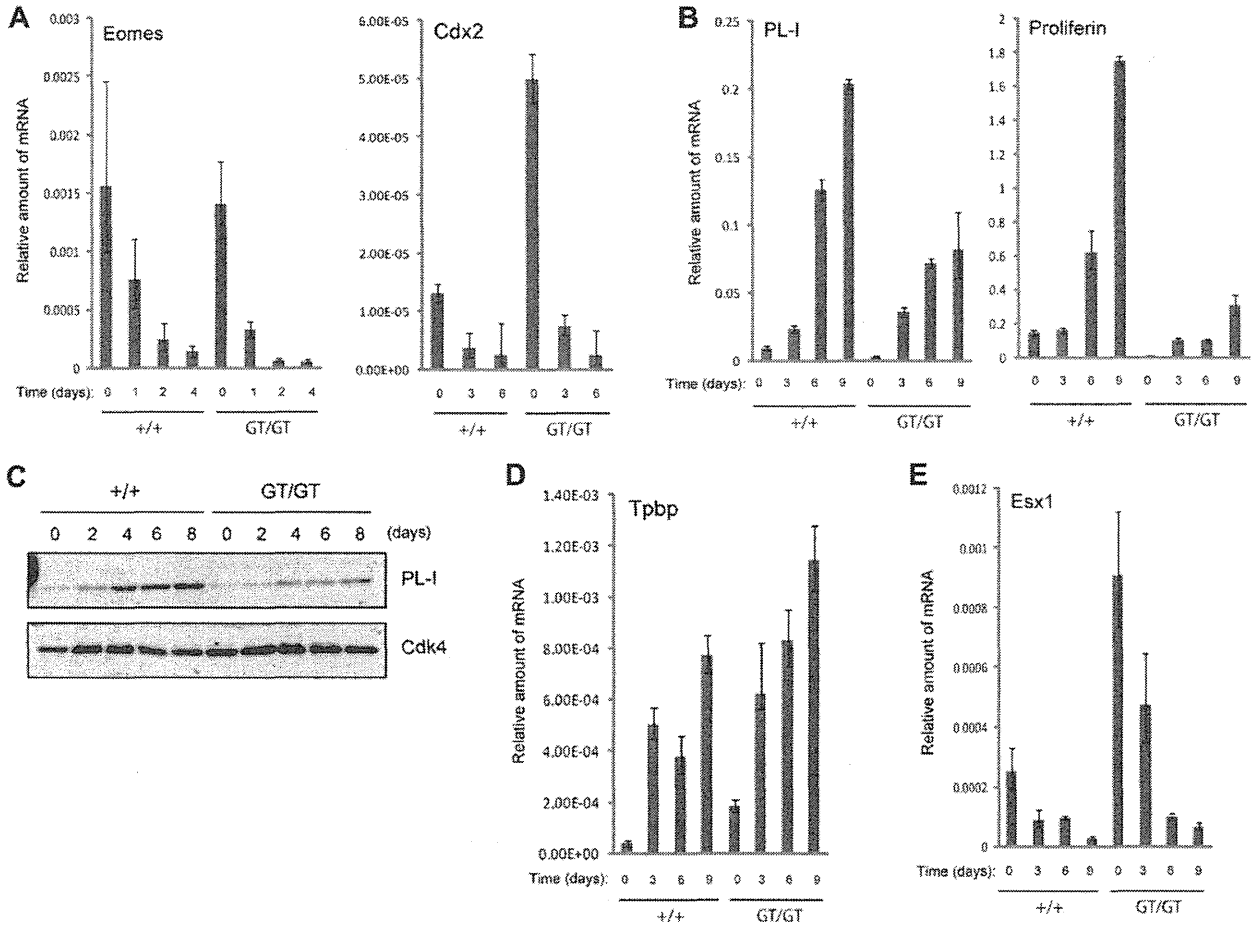

Fig. 3. Aberrant differentiation of *Cdh1*$^{GT/GT}$ TS cells into TG cells. (A–E) Wild-type and *Cdh1*$^{GT/GT}$ TS cells were incubated in the absence of F4H for the indicated times, and total RNA was isolated and subjected to quantitative RT-PCR analysis of mRNAs for Eomes or Cdx2 (A), PL-1 or Proliferin (B), Tpbp (D), or Esx1 (E). Data were normalized to the amount of ubiquitin mRNA and are represented as means ± SD from at least three independent experiments. (C) Immunoblot analysis of PL-1 protein levels in cells incubated in the absence of F4H for the indicated times. Expression of Cdk4 was used as a protein loading control.

in *Cdh1*$^{GT/GT}$ cells even after 5 days of F4H deprivation (Fig. 2A and C), and *Cdh1*$^{GT/GT}$ cells typically did not stop proliferating after F4H deprivation (Fig. 2D). These results strongly suggest that *Cdh1*$^{GT/GT}$ TS cells fail to switch to the endocycle and continue to undergo precocious mitotic entry.

In *Drosophila*, Cdh1 regulates the mitotic/endocycle switch by mediating the destruction of mitotic cyclins [4,5]. To address whether such a mechanism is conserved in mammals, the expression of mitotic cyclins and other Cdh1-targets was examined in TS cells after F4H depletion. Mitotic cyclins (Cyclin A and Cyclin B) accumulated in *Cdh1*$^{GT/GT}$ cells during the early stages of induction of TS cell differentiation (Fig. 2E, first and second rows). Other targets of Cdh1, such as Skp2 and Aurora A [19,20], also accumulated in *Cdh1*$^{GT/GT}$ cells (Fig. 2E, fifth and sixth rows). Contrary, the expression of p27 in *Cdh1*$^{GT/GT}$ cells was slightly reduced when compared with that in wild-type cells, which might be due to accumulation of Skp2, a ubiquitin ligase that targets p27 [21] (Fig. 2E, seventh and fifth rows). These results suggested that the accumulation of mitotic cyclins (and possibly a decrease in the CDK inhibitor) led to precocious mitotic entry in *Cdh1*$^{GT/GT}$ cells.

3.3. Abnormal differentiation of *Cdh1*$^{GT/GT}$ TS cells

To determine whether the abnormal proliferative potential of *Cdh1*$^{GT/GT}$ TS cells affects their differentiation into TG cells, RT-PCR and real-time PCR analyses were used to examine the expression of differentiation markers characteristic of the different trophoblast cell lineages. Culture of both wild-type and *Cdh1*$^{GT/GT}$ TS cells in the absence of F4H resulted in loss of mRNAs encoding the stem cell markers eomesodermin (Eomes) and Cdx2 (Fig. 3A). By contrast, up-regulation of the mRNAs for the TG cell differentiation markers placental lactogen-1 (PL-1) and proliferin (Plf-1) was markedly suppressed in *Cdh1*$^{GT/GT}$ cells compared to wild-type cells (Fig. 3B). Consistent with this difference in mRNA abundance, the amount of PL-1 protein in wild-type cells was much greater than that of *Cdh1*$^{GT/GT}$ cells (Fig. 3C). By contrast, expression of the spongiotrophoblast marker Tpbp (also known as 4311) was greater in *Cdh1*$^{GT/GT}$ cells compared to wild-type cells (Fig. 3D). The level of transcripts encoding the labyrinth layer marker Esx1 was greater in *Cdh1*$^{GT/GT}$ cells at early time points compared to wild-type cells (Fig. 3E). These results indicate that Cdh1 deficiency results in abnormal TG cell differentiation *in vitro*. In contrast with previous observations that showed a separation of endoreplication and differentiation in TG cells [17,22], loss of Cdh1 affected both processes.

To confirm the data obtained by RT-PCR and real-time PCR analyses of the expression of trophoblast differentiation marker genes, *in situ* hybridization was performed to evaluate TG cell differentiation *in vivo*. Transcripts for the TG cell differentiation marker proliferin showed a cytoplasmic staining pattern in cells with large nuclei in wild-type placentas (Fig. 4A), consistent with previous observations [23]. By contrast, the staining was almost completely absent in *Cdh1*$^{GT/GT}$ placentas (Fig. 4B), which suggested that the *in vivo* differentiation of TG cells was compromised in the gene-trapped animals.

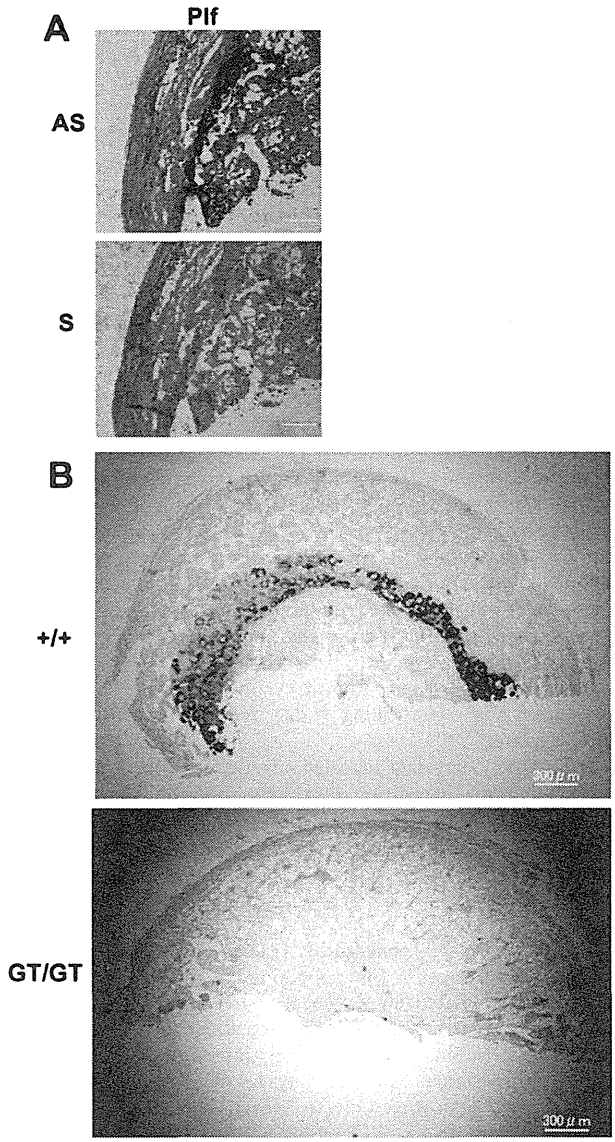

Fig. 4. Reduced expression of a TG cell specific marker in the placenta of *Cdh1*$^{GT/GT}$ embryos. *In situ* hybridization analysis of proliferin mRNA in sections of E12.5 (A) and E10.5 (B) placenta. (A) Panels show staining of wild-type placenta with antisense (AS, upper panel) or sense (S, lower panel) probes. (B) Upper and lower panels show wild-type and *Cdh1*$^{GT/GT}$ placentas (E10.5) stained with the antisense probe. The counterstain was methyl green. Scale bars, 300 μm. (For interpretation of the references to color in this figure legend, the reader is referred to the web version of this article.)

4. Discussion

In the present study, Cdh1 was shown to function in the mitotic/endocycle transition in TS cells. *Cdh1*$^{GT/GT}$ TS cells could not block mitosis when differentiated into TG cells by F4H deprivation, resulting in endocycle failure (Fig. 2C and D). Cdh1 suppressed mitotic entry via degradation of mitotic cyclins (Fig. 2E). Similarly, *Drosophila Cdh1* mutant follicle and nurse cells could not switch from the mitotic cycle to the endocycle as a result of accumulation of mitotic cyclins [4,5]. Therefore, the role of Cdh1 in the mitotic/endocycle transition is well conserved from fly to mammals.

Cdk1 activity is required for entry into mitosis [24]. To prevent segregation of damaged and/or improperly replicated chromosomes, Cdk1 activity is strictly regulated by several distinct but highly conserved mechanisms [25–27]. Recent studies indicate that Cdh1 plays a role in mitotic entry as a part of the DNA damage-induced G2 checkpoint [28,29]. Upon double-strand DNA breaks, the Cdc14B phosphatase is released from the nucleolus into the nucleoplasm, where Cdc14B dephosphorylates and activates Cdh1 to target the polo-like kinase1 (PLK1) for degradation. Since PLK1 antagonizes ATR/Chk1/Cdc25A signaling, Cdh1 enhances the Chk1-mediated Cdk1 inhibition after DNA damage in G2 [29].

Therefore, Cdh1 is involved in the G2/M transition in DNA-damaged cells. Given that Cdh1 participates in mitotic exit via Cyclin B degradation (Cdk1 inhibition) in the unperturbed mitotic cell cycle, Cdh1-mediated signaling pathways control Cdk1 activity not only at mitotic exit but also at mitotic entry.

Importantly, Cdh1-mediated regulation of the G2/M transition is not restricted to TS cell differentiation or the DNA damage checkpoint of somatic cells. In mammals, oocytes are arrested at the dictyate prophase I, equivalent to the G2 phase [30]. Oocytes resume the cell cycle to enter meiotic metaphase I after a peri-ovulatory luteinizing hormone surge. Cdh1 promotes Cyclin B degradation to inhibit precocious meiotic entry before a hormonal cue [30]. Collectively, Cdh1 has many physiological roles that are well correlated with the control of the G2/M transition via its regulation of Cdk1 activity.

Cdk1 suppression is required for the mitotic/endocycle transition and TS cell differentiation. Ullah et al. reported that the CDK1 inhibitor p57 can induce TS cells to differentiate into TG cells, which showed that suppression of Cdk1 is an essential step in TS cell differentiation [6]. In this study, we could not clearly detect the reduced levels of p57 in *Cdh1*$^{GT/GT}$ TS cells after F4H deprivation (Fig. 2E, eighth row). However, mitotic cyclins were significantly accumulated in these cells (Fig. 2E, first and second rows), suggesting Cdk1 can be inhibited by another means. Indeed, we found *Cdh1*$^{GT/GT}$ TS cells and placenta showed defective expression of placental differentiation markers (Figs. 3 and 4). Thus, post-translational regulation of mitotic cyclins comprises an important mechanism for controlling Cdk1 activity during TS cell differentiation.

In summary, our data revealed a conserved role of Cdh1 in the mitotic/endocycle transition. Cdh1 regulated the G2/M transition to facilitate a switch from mitosis to the endocycle and also participated in TS cell differentiation during placental development.

Acknowledgments

We thank Drs. G. Leone and P. L. Wenzel for providing *in situ* hybridization probes; N. Tomotsugu for assistance in the statistical analyses; I. Ishimatsu for technical assistance in the histological analysis; T. Shinoda for technical assistance in the analysis of nuclear size; N. Suzuki for animal maintenance; and K. Arai for secretarial assistance. This study was supported by grants from the Ministry of Education, Culture, Sports, Science, and Technology (MEXT) of Japan (to S.K. (20058033) and H.S. (17013070)).

References

[1] B.A. Edgar, T.L. Orr-Weaver, Endoreplication cell cycles: more for less, Cell 105 (2001) 297–306.
[2] H.O. Lee, J.M. Davidson, R.J. Duronio, Endoreplication: polyploidy with purpose, Genes Dev. 23 (2009) 2461–2477.
[3] M.A. Lilly, R.J. Duronio, New insights into cell cycle control from the Drosophila endocycle, Oncogene 24 (2005) 2765–2775.
[4] S.J. Sigrist, C.F. Lehner, Drosophila fizzy-related down-regulates mitotic cyclins and is required for cell proliferation arrest and entry into endocycles, Cell 90 (1997) 671–681.
[5] V. Schaeffer, C. Althauser, H.R. Shcherbata, W.M. Deng, H. Ruohola-Baker, Notch-dependent Fizzy-related/Hec1/Cdh1 expression is required for the mitotic-to-endocycle transition in Drosophila follicle cells, Curr. Biol. 14 (2004) 630–636.
[6] Z. Ullah, M.J. Kohn, R. Yagi, L.T. Vassilev, M.L. DePamphilis, Differentiation of trophoblast stem cells into giant cells is triggered by p57/Kip2 inhibition of CDK1 activity, Genes Dev. 22 (2008) 3024–3036.
[7] P. Zhang, C. Wong, R.A. DePinho, J.W. Harper, S.J. Elledge, Cooperation between the Cdk inhibitors p27(KIP1) and p57(KIP2) in the control of tissue growth and development, Genes Dev. 12 (1998) 3162–3167.
[8] K. Takahashi, T. Kobayashi, N. Kanayama, P57(Kip2) regulates the proper development of labyrinthine and spongiotrophoblasts, Mol. Hum. Reprod. 6 (2000) 1019–1025.
[9] I. Garcia-Higuera, E. Manchado, P. Dubus, M. Canamero, J. Mendez, S. Moreno, M. Malumbres, Genomic stability and tumour suppression by the APC/C cofactor Cdh1, Nat. Cell Biol. 10 (2008) 802–811.
[10] M. Li, Y.H. Shin, L. Hou, X. Huang, Z. Wei, E. Klann, P. Zhang, The adaptor protein of the anaphase promoting complex Cdh1 is essential in maintaining replicative lifespan and in learning and memory, Nat. Cell Biol. 10 (2008) 1083–1089.
[11] H. Naoe, K. Araki, O. Nagano, Y. Kobayashi, J. Ishizawa, T. Chiyoda, T. Shimizu, K. Yamamura, Y. Sasaki, H. Saya, S. Kuninaka, The anaphase-promoting complex/cyclosome activator Cdh1 modulates Rho GTPase by targeting p190 RhoGAP for degradation, Mol. Cell. Biol. 30 (2010) 3994–4005.
[12] S. Tanaka, T. Kunath, A.K. Hadjantonakis, A. Nagy, J. Rossant, Promotion of trophoblast stem cell proliferation by FGF4, Science 282 (1998) 2072–2075.
[13] M. Oda, K. Shiota, S. Tanaka, Trophoblast stem cells, Methods Enzymol. 419 (2006) 387–400.
[14] S. Kuninaka, S.I. Iida, T. Hara, M. Nomura, H. Naoe, T. Morisaki, M. Nitta, Y. Arima, T. Mimori, S. Yonehara, H. Saya, Serine protease Omi/HtrA2 targets WARTS kinase to control cell proliferation, Oncogene 26 (2007) 2395–2406.
[15] S. Noji, T. Yamaai, E. Koyama, T. Nohno, W. Fujimoto, J. Arata, S. Taniguchi, Expression of retinoic acid receptor genes in keratinizing front of skin, FEBS Lett. 259 (1989) 86–90.
[16] L. Wu, A. de Bruin, H.I. Saavedra, M. Starovic, A. Trimboli, Y. Yang, J. Opavska, P. Wilson, J.C. Thompson, M.C. Ostrowski, T.J. Rosol, L.A. Woollett, M. Weinstein, J.C. Cross, M.L. Robinson, G. Leone, Extra-embryonic function of Rb is essential for embryonic development and viability, Nature 421 (2003) 942–947.
[17] T. Parisi, A.R. Beck, N. Rougier, T. McNeil, L. Lucian, Z. Werb, B. Amati, Cyclins E1 and E2 are required for endoreplication in placental trophoblast giant cells, EMBO J. 22 (2003) 4794–4803.
[18] R. Sigl, C. Wandke, V. Rauch, J. Kirk, T. Hunt, S. Geley, Loss of the mammalian APC/C activator FZR1 shortens G1 and lengthens S phase but has little effect on exit from mitosis, J. Cell Sci. 122 (2009) 4208–4217.
[19] J.M. Peters, The anaphase promoting complex/cyclosome: a machine designed to destroy, Nat. Rev. Mol. Cell Biol. 7 (2006) 644–656.
[20] J. Pines, Cubism and the cell cycle: the many faces of the APC/C, Nat. Rev. Mol. Cell Biol. 12 (2011) 427–438.
[21] A.C. Carrano, E. Eytan, A. Hershko, M. Pagano, SKP2 is required for ubiquitin-mediated degradation of the CDK inhibitor p27, Nat. Cell Biol. 1 (1999) 193–199.
[22] R.L. Gardner, T.J. Davies, Lack of coupling between onset of giant transformation and genome endoreduplication in the mural trophectoderm of the mouse blastocyst, J. Exp. Zool. 265 (1993) 54–60.
[23] D.G. Simmons, A.L. Fortier, J.C. Cross, Diverse subtypes and developmental origins of trophoblast giant cells in the mouse placenta, Dev. Biol. 304 (2007) 567–578.
[24] A. Lindqvist, V. Rodriguez-Bravo, R.H. Medema, The decision to enter mitosis: feedback and redundancy in the mitotic entry network, J. Cell Biol. 185 (2009) 193–202.
[25] J.W. Harper, S.J. Elledge, The DNA damage response: ten years after, Mol. Cell 28 (2007) 739–745.
[26] J. Bartek, J. Lukas, DNA damage checkpoints: from initiation to recovery or adaptation, Curr. Opin. Cell Biol. 19 (2007) 238–245.
[27] D.O. Morgan, Principles of CDK regulation, Nature 374 (1995) 131–134.
[28] T. Sudo, Y. Ota, S. Kotani, M. Nakao, Y. Takami, S. Takeda, H. Saya, Activation of Cdh1-dependent APC is required for G1 cell cycle arrest and DNA damage-induced G2 checkpoint in vertebrate cells, EMBO J. 20 (2001) 6499–6508.
[29] F. Bassermann, D. Frescas, D. Guardavaccaro, L. Busino, A. Peschiaroli, M. Pagano, The Cdc14B-Cdh1-Plk1 axis controls the G2 DNA-damage-response checkpoint, Cell 134 (2008) 256–267.
[30] J.E. Holt, J. Weaver, K.T. Jones, Spatial regulation of APCCdh1-induced cyclin B1 degradation maintains G2 arrest in mouse oocytes, Development 137 (2010) 1297–1304.

肝癌予防の基礎と臨床

渡邊 丈久・田中 基彦・佐々木 裕

キーポイント

☆慢性肝疾患の進展の程度と肝発癌の頻度には正の相関がある.

☆肝癌の進展には多因子の関与が想定される.

☆肝の前癌病変では,活性酸素種(ROS),活性化誘導シチジンデアミナーゼ(AID),エピジェネティクス変化による遺伝子発現異常が蓄積している.

肝での多段階発癌

多段階発癌とは,いくつもの遺伝子変異や発現の異常が積み重なって,細胞が次第に悪性化し,癌化する過程をさす.肝細胞癌(以下,肝癌)では,C型肝炎ウイルス,B型肝炎ウイルスの感染,アルコール多飲,メタボリック症候群などから生じた肝硬変が,非常に癌が発生しやすい状況である前癌状態として捉えることができる.このような状況では,まず組織学的な前癌状態である異型結節が生じ,癌細胞としての生物学的特性を獲得すると早期癌に変化する.さらに悪性度が増すと進行肝癌となる.

C型慢性肝炎からの肝硬変への進展過程では,肝線維化と年次発癌率に明らかな正の相関があり,肝疾患を進展させる炎症を制御することは肝発癌に対する最大の防御となる.

肝癌で発現が変化する遺伝子とそれらが関与する経路

肝癌に限らず,一般的に発癌過程では癌遺伝子の活性化,もしくは癌抑制遺伝子の不活性化が重要である.現在,肝癌で確認されている遺伝子変異の知見より,p53関連遺伝子群や*RB*や*INK4a*,核内にβ-catenin蓄積を伴うWntシグナル関連遺伝子群が重要であると考えられている(表1).また,代謝性疾患との関連が疑われるPI3K/Akt経路やRas/MAPK経路,さらに各種炎症性サイトカインと関与するNF-κB経路などの関連も注目されている.

最近ではゲノムの網羅的解析により,慢性肝炎からの発癌に特徴的な一塩基多型(SNPs)が報告された[1].肝癌の進展には多因子の関与が想定されるため,単一の遺伝子変異ではなく,多くの遺伝子発現や中間代謝物を網羅的に解析して得られる情報を統合したパスウェイ解析が重要である.一方,全ヒトゲノム解読により生命科学の急速な進歩に貢献した国際ヒトゲノム計画に続くポストゲノムプロジェクトとして,現在,主要な癌のゲノム変異カタログを作成する「国際癌ゲノムコンソーシアム(International Cancer Genome Consortium:ICGC)」が世界各国の協力で進行中である.日本が担当した肝

わたなべ たけひさ・たなか もとひこ・ささき ゆたか:熊本大学大学院生命科学研究部消化器内科学分野 〒860-8556 熊本市本荘1-1-1

0025-7699/12/¥500/包文/JCOPY